

Brain Maturation in Adolescence: Concurrent Changes in Neuroanatomy and Neurophysiology

Thomas J. Whitford,^{1,2*} Christopher J. Rennie,^{1,3} Stuart M. Grieve,⁴
C. Richard Clark,⁵ Evian Gordon,^{1,4,6} and Leanne M. Williams^{1,6}

¹Brain Dynamics Centre, Westmead Millennium Institute and University of Sydney, Westmead Hospital, New South Wales, Australia

²School of Psychology, University of Sydney, New South Wales, Australia

³Department of Medical Physics, Westmead Hospital, New South Wales, Australia

⁴Brain Resource International Database, Sydney, New South Wales, Australia

⁵Cognitive Neuroscience Laboratory and School of Psychology, Flinders University, Adelaide, South Australia, Australia

⁶Department of Psychological Medicine, University of Sydney, New South Wales, Australia



Abstract: Adolescence to early adulthood is a period of dramatic transformation in the healthy human brain. However, the relationship between the concurrent structural and functional changes remains unclear. We investigated the impact of age on both neuroanatomy and neurophysiology in the same healthy subjects (n = 138) aged 10 to 30 years using magnetic resonance imaging (MRI) and resting electroencephalography (EEG) recordings. MRI data were segmented into gray and white matter images and parcellated into large-scale regions of interest. Absolute EEG power was quantified for each lobe for the slow-wave, alpha and beta frequency bands. Gray matter volume was found to decrease across the age bracket in the frontal and parietal cortices, with the greatest change occurring in adolescence. EEG activity, particularly in the slow-wave band, showed a similar curvilinear decline to gray matter volume in corresponding cortical regions. An inverse pattern of curvilinearly increasing white matter volume was observed in the parietal lobe. We suggest that the reduction in gray matter primarily reflects a reduction of neuropil, and that the corresponding elimination of active synapses is responsible for the observed reduction in EEG power. *Hum Brain Mapp* 28:228–237, 2007. © 2006 Wiley-Liss, Inc.

Key words: adolescence; maturation; magnetic resonance imaging; electroencephalography; gray matter; white matter; slow-wave power



INTRODUCTION

While the most dramatic structural changes in the healthy human brain are thought to occur in the perinatal period [Huttenlocher and Dabholkar, 1997], there is a growing body of evidence suggesting that adolescence is also a period of substantial neurodevelopment [Sisk and Foster, 2004]. Research into brain maturation over adolescence and early adulthood is particularly important, given that it is a peak period of neural reorganization that contributes to both normal variation and the onset of major mental illnesses, such as schizophrenia [Keshavan et al., 1994]. Despite growing evidence for pronounced changes in both the structure

*Correspondence to: Thomas J. Whitford, Brain Dynamics Centre, Acacia House, Westmead Hospital, Westmead, NSW, 2145, Australia. E-mail: twhi4033@mail.usyd.edu.au

Received for publication 10 November 2005; Accepted 22 February 2006

DOI: 10.1002/hbm.20273

Published online 9 June 2006 in Wiley InterScience (www.interscience.wiley.com).

and function of the brain during adolescence and early adulthood, the relationship between these changes has not been directly examined. The objective of this study was to examine these concurrent developmental changes by obtaining both neuroanatomical measures of structural change (with magnetic resonance imaging, MRI) and electroencephalographic indexes of neural function for the first time in a large sample ($n = 138$) of healthy subjects.

A number of MRI studies have reported an intense period of gray matter tissue loss in the peripubescent period between 10 and 18 years of age [Pfefferbaum et al., 1994; Steen et al., 1997; Giedd et al., 1999]. This gray matter loss, which appears to occur most severely in the association cortices [Sowell et al., 1999], is thought not to be primarily due to neuron death, but rather due to the elimination of naturally overproduced synapses and their associated neuropil (dendrites, dendritic spines, and axon terminals) [Purves, 1998]. Increased competition for trophic factors in target cells, possibly mediated by hormonal influences, has been proposed as a cause for this "synaptic prune" [Purves and Lichtman, 1980]. Regarding white matter, previous studies have reported increases in white matter volume over the peripubescent period, especially in the frontal lobe and hippocampal relays [Benes, 1989; Benes et al., 1994]. This white matter gain, which is thought to reflect increased axonal myelination [Paus et al., 2001], has been associated with the development of language and memory skills in adolescence [Nagy et al., 2005].

Complementing the neuroanatomical studies, changes in brain function during adolescence have been investigated by electrophysiological means. Matousek and Petersen [1973], for example, measured changes in the electroencephalogram (EEG) in a large group ($n = 348$) of adolescents/young adults aged 10 to 20 years and found that absolute EEG power decreased in all frequency bands, particularly in the slow-wave band of below 7.5 Hz. This finding has since been replicated [Matsuura et al., 1985; Gasser et al., 1988]. This decrease has been found to continue into adulthood, albeit at a lesser rate than in adolescence [Dustman et al., 1999].

The EEG signal is thought to arise from areas of spatially coherent synaptic activity at the cortex [Niedermeyer and Lopes de Silva, 1999], with absolute EEG power being related to the amplitudes of the resultant waves in scalp electrical potential. It might be expected, therefore, that a dramatic reduction in the number of cortical synapses in adolescence would correspond to a substantial reduction in absolute EEG power. While this relationship has not been explicitly examined, Feinberg [1982] alluded to the idea when he noted that Huttenlocher's [1979] data of synaptic density in the cerebral cortex showed a similar trend across age to his own data on slow-wave EEG power in sleep, with both showing a steep reduction in early adolescence. Evidence for a gray matter-EEG relationship, independent of age, comes from head-injured patients with gray matter atrophy, who show a corresponding decrease in EEG amplitude, especially in the alpha and beta bands [Thatcher et al., 1998]. However, to our knowledge, no previous studies

TABLE I. Breakdown of the subject sample in terms of age and gender

	Age bracket (years)						Total
	10-14	15-17	18-19	20-21	22-24	25-29	
Number of men	8	8	11	11	12	20	70
Number of women	11	11	11	7	12	16	68
Total	19	19	22	18	24	36	138

have directly investigated the relationship between the anatomical and electrophysiological brain changes that occur in adolescence and early adulthood.

In this study, we examined both structural MRI and concurrent quantified EEG in healthy subjects aged between 10 and 30 years. We anticipated that subjects' gray matter volume would decrease curvilinearly over this period, especially in the frontal and parietal regions, reflecting the extended maturation of these association cortices. A corresponding decrease in absolute power was expected for the EEG data in the corresponding cortical regions. On the other hand, it was hypothesized that white matter volume would increase curvilinearly across this period, again most apparently in the frontal and parietal lobes. It was expected that the greatest differences in both neuroanatomy and neurophysiology would be apparent during adolescence before reaching an asymptote in the mid-20s.

MATERIALS AND METHODS

Participants

One hundred thirty-eight healthy participants (70 female, 68 male), distributed evenly between 10 and 30 years of age (Table I), were recruited from the Brain Resource International Database (BRID; <http://www.brainresource.com>). Exclusion criteria included a personal history of mental illness, physical brain injury, neurological disorder or other serious medical condition, and/or a personal history of drug or alcohol addiction. The SPHERE questionnaire [Hickie et al., 1998] was used to screen for likely Axis-1 psychiatric disorder. All subjects (or their guardians for subjects less than 18 years of age) provided written informed consent to participate in the database. Subjects were required to refrain from caffeine intake and from smoking for at least 2 hr prior to the EEG testing.

MR Imaging and Parcellation

All subjects underwent a single T1-weighted volumetric MPRAGE structural MRI scan on a Siemens 1.5 Tesla Vision Plus system at Westmead Hospital, Sydney, Australia. Images were obtained in the sagittal plane, with scan parameters time to repeat (TR) = 9.7 ms, time to echo (TE) = 4 ms, inversion time (TI) = 200 ms, flip angle = 12°. A total of 180 contiguous 1-mm slices were acquired with a 256 × 256 matrix with an in-plane resolution of 1 mm × 1 mm, resulting in isotropic voxels.

Images were processed using SPM2 (Wellcome Department of Cognitive Neurology, London, United Kingdom), running on MATLAB 6.5 (MathWorks, Natick, MA). The full details of the processing protocol used in voxel-based morphometry (VBM) are presented elsewhere [Ashburner and Friston, 2000; Good et al., 2001]. Briefly, subject brain images were first spatially normalized by transforming each brain into a standardized stereotactic space based on the ICBM 152 template (Montreal Neurological Institute) that approximates Talairach space. This process was performed using a custom T1 image template using 333 brain images from the BRID that were acquired using the same protocol. The first step in spatial normalization involved estimating the optimum 12-parameter affine transformation (3 translations, 3 rotations, 3 zooms, and 3 shears) for matching the subject's image to the template. The second step accounted for global nonlinear shape differences, which were modeled by a linear combination ($7 \times 8 \times 7$) of smooth spatial basis functions [Ashburner and Friston, 2000]. The normalized images were resliced with $1.5 \times 1.5 \times 1.5$ mm voxels, before being segmented into gray matter (GM), white matter (WM), and cerebrospinal fluid (CSF) probability maps and stripped of extracerebral voxels. Segmentation was based on a cluster analysis method that accounted for each voxel's signal intensity, together with an a priori expectation of the anatomical location of the different tissue types. In order to adjust for the growth and shrinkage of voxels that can occur during spatial normalization, voxel probability values in the cleaned segmented images were modulated with the Jacobean determinants derived from the spatial normalization [Good et al., 2001]. Thus, if a brain region doubled in size as a result of normalization, the gray matter probability value for this region would be halved for the purposes of calculating its volume [Ashburner and Friston, 2001]. The processed GM, WM, and CSF images were smoothed with a Gaussian kernel of 12 mm full width at half maximum prior to volume calculation.

The preprocessed gray and white matter images were then automatically parcellated into regions of interest (ROIs). Five GM supregions (frontal, parietal, temporal, occipital, and limbic lobes) were parcellated using the previously published Automatic Anatomical Labeling (AAL) masks [Tzourio-Mazoyer et al., 2002] as listed in Table II and illustrated in Figure 1. The AAL parcellation was chosen as the basis for the segmentation because it is defined in Montreal Neurological Institute (MNI) space, which is a standardized coordinate system in common usage. Parcellation was performed in an axial view, and assignments were cross-checked with AAL parcellation to ensure consistency. The frontal lobe was defined as all cerebrum anterior to the central sulcus and superior to the sylvian fissure. At the deepest point of the central sulcus, a straight line was drawn to the interhemispheric fissure. In planes where the anterior horns of the lateral ventricles were visible, a line was drawn from the central sulcus to the anterior limit of the ventricles, then back to the interhemispheric fissure. The corpus callosum was separately outlined to exclude it from the frontal

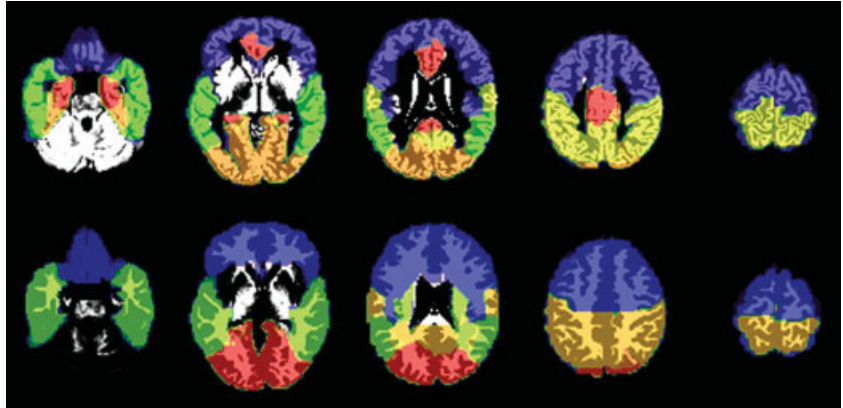
TABLE II. The 5 supregional gray matter masks and their constituent AAL masks

Frontal lobe
Precentral gyrus
Superior frontal gyrus, dorsolateral
Superior frontal gyrus, medial
Superior frontal gyrus, medial orbital
Superior frontal gyrus, orbital part
Middle frontal gyrus, orbital part
Middle frontal gyrus
Inferior frontal gyrus, opercular part
Inferior frontal gyrus, triangular part
Inferior frontal gyrus, orbital part
Rolandic operculum
Paracentral lobule
Supplementary motor area
Olfactory cortex
Gyrus rectus
Temporal lobe
Superior temporal gyrus
Temporal pole: superior temporal gyrus
Middle temporal gyrus
Temporal pole: middle temporal gyrus
Inferior temporal gyrus
Heschl gyrus
Limbic lobe
Anterior cingulate and paracingulate gyri
Median cingulate and paracingulate gyri
Posterior cingulate gyrus
Hippocampus
Parahippocampal gyrus
Amygdala
Occipital lobe
Cuneus
Lingual gyrus
Superior occipital gyrus
Middle occipital gyrus
Inferior occipital gyrus
Fusiform gyrus
Calcarine fissure and surrounding cortex
Parietal lobe
Postcentral gyrus
Superior parietal gyrus
Inferior parietal, minus supramarginal and angular gyri
Supramarginal gyrus
Angular gyrus
Precuneus

lobe. In slices containing the insula, with reference to the AAL parcellation, this region was excluded, and a line was drawn from the sylvian fissure to the interhemispheric fissure. Inferior regions of the brain were clearly separated from temporal lobe structures by CSF. The parietal lobe was traced in a sagittal plane defined as all cerebrum superior and anterior to the parieto-occipital sulcus, posterior to the central sulcus, and superior to the corpus callosum. The occipital lobe was defined as everything posterior to the boundaries described below. Parcellation of the occipital lobe was performed from the midline in a parasagittal view. The anterosuperior border was defined by the parieto-occipital and the temporo-occipital sulci. Lateral to the midline, from where the parieto-occipital sulcus was no longer prominent, a straight line was drawn between it and the horizontal ramus of the superior temporal sulcus. The posteroinfe-

Figure 1.

Illustration of the regions of interest identified for the structural MR images. The five gray matter regions of interest are shown on top, superimposed on the GM segment of the MNI T1-weighted single-subject brain. Blue, frontal; green, temporal; orange, occipital; yellow, parietal; red, limbic. The four white matter regions of interest are shown below, superimposed on the WM segment of the MNI single-subject image. Blue, frontal; green, temporal; orange, parietal; red, occipital.



rior border was defined by the anterior calcarine sulcus, the collateral sulcus, and the posterior transverse collateral sulcus and included the lingual gyrus. The temporal lobe included the superior, middle, and inferior gyri. The borders were defined by the sylvian fissure, occipitotemporal sulcus, superior temporal sulcus, and the lateral border of the parahippocampal gyrus. The limbic lobe was created by amalgamating the following discrete structures: cingulate and paracingulate gyri, amygdala, hippocampus, and parahippocampal gyrus.

Very few neuroanatomical studies have examined regional WM volumes due to the difficulty in distinguishing between various WM tracts when manually defining ROIs. An advantage of using a common set of masks for all subjects is that it is unbiased and ensures that the region of brain defined by the mask is consistent between subjects, assuming that global differences in brain shape have been largely removed by spatial normalization. The four WM masks used in this study are displayed in Figure 1. The WM ROIs were generated in MNI space, in consultation with a radiologist, and were defined with reference to the AAL model and a segmented WM image as follows. The corpus callosum and internal capsule were defined first, the external borders of these being used to limit the internal aspects of the frontal, parietal, and temporal lobes. The occipitoparietal border was interpolated from the borders of the superficial occipital and parietal lobes to the cuneus-precuneus border. The temporo-occipital border was similarly defined by the previously parcellated borders of the occipital and temporal lobes. The frontal lobe border followed the central sulcus superficially, with the internal border defined as anterior to the putamen and caudate at the level of the anterior commissure, and as anterior to the amygdala inferiorly.

Volumes for the five GM and four WM regions were calculated by summing the values of the constituent voxels following Jacobean modulation.

Electrophysiological Data Acquisition and Parcellation

EEG was acquired using an electrode cap (Quikcap; Neuroscan) with 28 sites using the 10–20 system of electrode

placement. Horizontal eye movements were recorded with electrodes placed 1.5 cm lateral to the outer canthus of each eye. Vertical eye movements were recorded with electrodes placed 3 mm above the middle of the left eyebrow and 1.5 cm below the middle of the left bottom eyelid. The impedance at each site was below 10 kOhms. Data were obtained continuously using a NuAmps system (Neuroscan), a DC amplifier with large dynamic range (± 132 mV and 22 bit resolution). Each channel was sampled at 500 Hz after low-pass filtering with attenuation of 40 dB per decade above 100 Hz. Data were corrected for eye movement offline [Gratton et al., 1983] and rereferenced to the average of A1 and A2 (mastoids). The EEG data reported and analyzed in the present study were recorded during a 2-min interval in

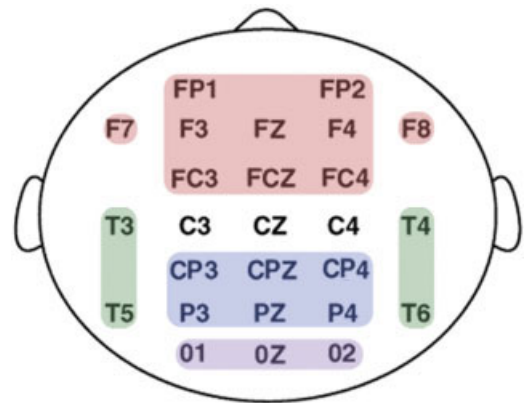


Figure 2.

Schematic diagram of the constituent electrodes of the four EEG regions. Electrodes making up the frontal lobe EEG region are in red, the temporal lobe EEG region in green, the parietal lobe EEG region in blue, and the occipital lobe EEG region in purple. The average power of each EEG region (for each frequency band for each subject) was calculated by averaging the standardized absolute power scores of the constituent electrodes.

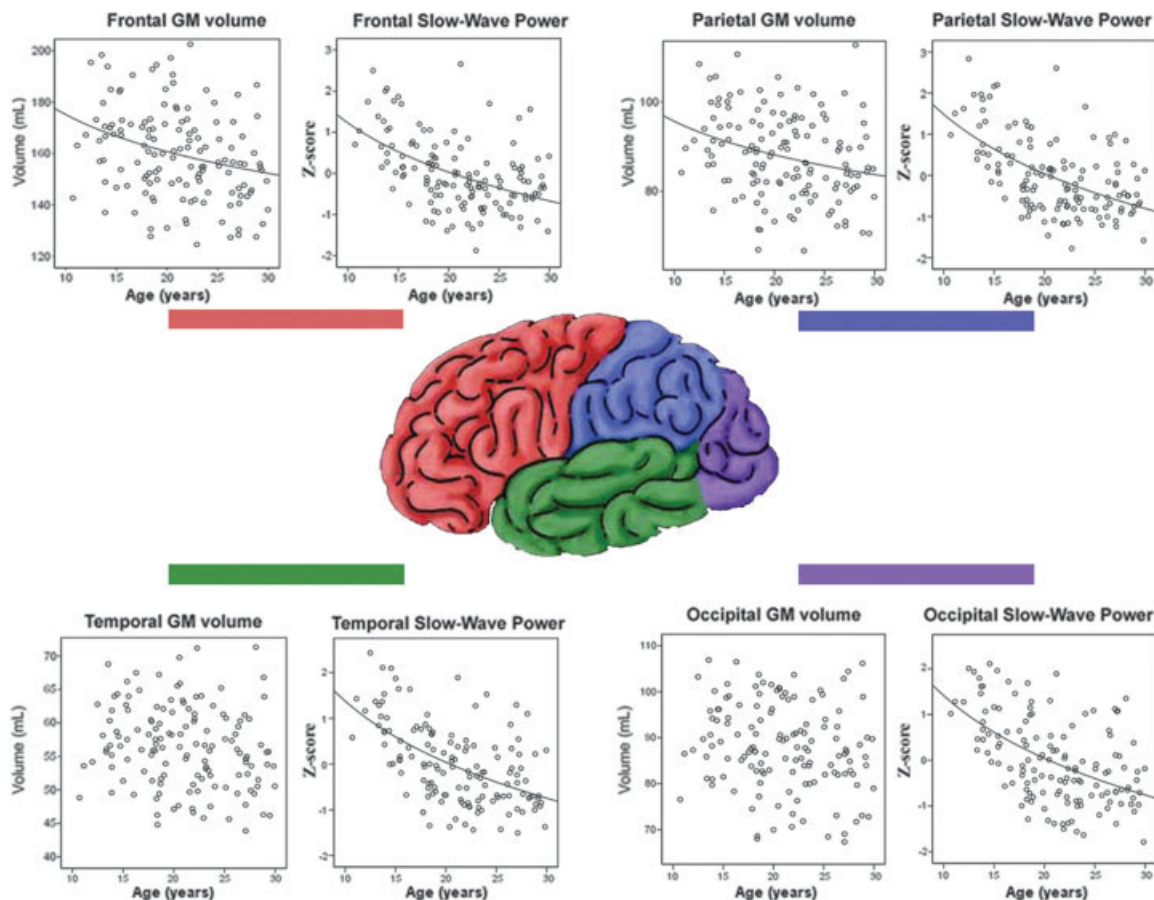


Figure 3. Gray matter vs. age scatterplots for the frontal, parietal, temporal, and occipital regions of interest.

which subjects were asked to rest quietly with their eyes closed.

Spectral power estimation was performed by first resampling the data at 512 Hz, before applying a Welch window to each successive 4-s epoch and then performing a fast Fourier transform (FFT). The resultant power spectra were averaged separately for each electrode. Power (in μV^2) was then calculated for three frequency bands—slow-wave (0.5–7.5 Hz), alpha (8–12 Hz), and beta (12.5–34.5 Hz)—and square-root-transformed in order that the values approximated the normal distribution required by parametric statistical methods.

To investigate the relationship between the change in neuroanatomical gray matter volume and the corresponding change in neural activity, we created four large-scale neural regions for the EEG (EEG regions) that corresponded to the four cortical GM regions. Neural activity over the frontal, parietal, temporal, and occipital lobes was calculated by averaging the standardized power recorded at each electrode site contributing to each region for slow-wave, alpha, and beta activity. For example, frontal lobe power for the alpha band was the average of standardized alpha power recorded from Fp1, Fp2, F7, F3, FZ, F4, F8, FC3, FCZ, and

FC4 electrode sites. A schematic diagram of the electrodes constituting the four EEG regions is given in Figure 2.

Statistical Analysis

Linear regression analyses were used to assess age-related trends in GM and WM volume and in the absolute power for the corresponding EEG regions. As we anticipated the rate of structural and functional brain change to be highest in adolescence before decreasing in the 20s, subjects' ages were logarithmically transformed before being entered as the predictor variable of interest. If the regression model was found to account for significant variance in the response variable (e.g., GM volume), the significance of the standardized regression coefficient (β) for the predictor variable [$\log(\text{age})$] was considered. Partial correlation analyses were used to assess the linear relationship between subjects' regional GM volumes and the averaged absolute power of their corresponding EEG regions. Due to the number of statistical comparisons made, an α level of 0.01 was used as the threshold for significance for all analyses. Sex was statistically controlled for in all analyses.

TABLE III. Linear regression analyses for the MR data, controlling for gender

MRI supraregion	β log(age)	t (β)	Sig (t)	R ² change log(age)	R ² model	F (model)	Sig (model)
Gray matter raw							
Frontal lobe	-0.229	-3.117	0.002	0.052	0.280	26.29	< 0.001
Temporal lobe	-0.110	-1.584	0.115	0.012	0.359	37.78	< 0.001
Parietal lobe	-0.227	-3.088	0.002	0.051	0.281	26.35	< 0.001
Occipital lobe	-0.088	-1.205	0.230	0.008	0.282	26.51	< 0.001
Limbic lobe	-0.088	-1.252	0.213	0.008	0.333	33.64	< 0.001
Subcortical	-0.089	-1.262	0.209	0.008	0.336	34.14	< 0.001
White matter raw							
Frontal lobe	0.194	2.451	0.016	0.037	0.187	15.05	< 0.001
Parietal lobe	0.214	2.808	0.006	0.046	0.244	21.15	< 0.001
Occipital lobe	0.173	2.340	0.021	0.030	0.285	26.06	< 0.001
Temporal lobe	0.195	2.594	0.011	0.038	0.260	23.06	< 0.001

Model: tissue volume = $b_0 + b_1(\text{gender}) + b_2[\log(\text{age})]$.

RESULTS

Gray matter volume was found to reduce linearly with the log of age in the frontal and parietal lobe supraregions. The log of age was not found to be a significant predictor of tissue volume in the temporal, occipital, or limbic GM supraregions (Fig. 3, Table III).

Absolute EEG power was also found to decrease linearly with the log of age for each of the three frequency bands across each of the four cortical EEG regions, i.e., frontal, temporal, parietal, and occipital lobe. The regression model was found to fit the age-related reduction of the slow-wave frequency band far better than it did the alpha or beta bands (Table IV). Scatterplots describing the change in slow-wave EEG power across age for the four EEG regions can be seen in Figure 3.

The hypothesized relationship between the number of active synapses and absolute EEG power was supported

by the significant positive correlations between subjects' GM volumes and their corresponding regional powers, particularly in the slow-wave frequency band [Table V; similar results were observed for all analyses when the slow-wave band was separated into the delta (0.5–3 Hz) and theta (3.5–7 Hz) frequency bands]. However, when we entered both slow-wave power and GM volume into the same regression analysis (controlling for sex), slow-wave power was found to be a substantially better predictor of log(age) than was GM volume for both the frontal ($\beta = -0.47$, $t = -5.87$, $P < 0.001$ vs. $\beta = -0.1$, $t = -1.13$, $P > 0.05$) and parietal ($\beta = -0.54$, $t = -6.95$, $P < 0.001$ vs. $\beta = -0.06$, $t = -0.71$, $P > 0.05$) lobes. Thus, the age-related changes in frontal and parietal GM volume and slow-wave EEG power, while mirroring each other in shape, were not completely parallel due to the increased variability of the GM data.

TABLE IV. Linear regression analyses for the absolute EEG power data, controlling for sex

EEG region	β log(age)	t (β)	Sig (t)	R ² change log(age)	R ² model	F (model)	Sig (model)
Slow-wave							
Frontal lobe	-0.5	-6.686	< 0.001	0.237	0.507	23.20	< 0.001
Temporal lobe	-0.57	-8.010	< 0.001	0.312	0.569	32.37	< 0.001
Parietal lobe	0.556	-7.750	< 0.001	0.294	0.316	31.02	< 0.001
Occipital lobe	-0.525	-7.122	< 0.001	0.272	0.273	25.40	< 0.001
Alpha							
Frontal lobe	-0.176	-2.059	0.041	0.03	0.031	2.151	0.120
Temporal lobe	-0.310	-3.765	< 0.001	0.094	0.095	7.092	0.001
Parietal lobe	-0.258	-3.072	0.003	0.065	0.066	4.725	0.010
Occipital lobe	-0.275	-3.313	0.001	0.079	0.082	6.043	0.003
Beta							
Frontal lobe	-0.226	-2.739	0.007	0.042	0.093	6.88	0.001
Temporal lobe	-0.310	-3.838	< 0.001	0.084	0.126	9.76	< 0.001
Parietal lobe	-0.255	-3.136	0.002	0.064	0.124	9.48	< 0.001
Occipital lobe	-0.361	-4.54	< 0.001	0.116	0.157	12.58	< 0.001

Model: regional power = $b_0 + b_1(\text{sex}) + b_2[\log(\text{age})]$.

TABLE V. Partial correlations (controlling for gender) between the volumes of the GM supraregions for the frontal, parietal, temporal, and occipital lobes and the absolute power of the corresponding EEG regions (e.g., frontal lobe GM with frontal lobe EEG power) for the slow-wave, alpha and beta frequency bands

MRI GM supraregions	Absolute power for the corresponding EEG regions		
	Slow-wave (<i>P</i>)	Alpha (<i>P</i>)	Beta (<i>P</i>)
Frontal	0.350 (< 0.001)	0.249 (0.003)	0.204 (0.017)
Temporal	0.214 (0.013)	0.235 (0.006)	0.102 (0.236)
Parietal	0.364 (< 0.001)	0.262 (0.002)	0.235 (0.006)
Occipital	0.345 (< 0.001)	0.295 (< 0.001)	0.274 (0.001)

White matter volume was found to increase linearly with the log of age only in the parietal WM ROI, although the log of age was close to being a statistically significant predictor of tissue volume in the remaining three WM ROIs (i.e., frontal, temporal, and occipital), with the α level set at 0.01 (Fig. 4, Table III).

DISCUSSION

The primary purpose of this study was to investigate the structural and electrophysiological brain changes associated with healthy adolescence and to examine the relationship between these changes. To this end, we recorded structural MRI and resting EEG from 138 healthy participants aged between 10 and 30 years. After controlling for the effects of sex, gray matter volume was found to be negatively correlated with the log of age in the frontal and parietal cortices, while white matter volume was found to be positively correlated with the log of age in the parietal lobe. Absolute EEG power, which was averaged over the frontal, temporal, parietal, and occipital cortices, was found to be negatively correlated with the log of age in all four EEG regions for each of the three frequency bands, but most strongly in the slow-wave band. This age-related reduction in slow-wave power mirrored the age-related reduction in GM volume, especially for the frontal and parietal cortices (Fig. 3). This finding was supported by the observed positive correlation between subjects' frontal and parietal GM volumes and the absolute power of their corresponding EEG regions (Table V). Our results provide evidence that changes in neural activity follow a similar trajectory to changes in brain structure over adolescence, at least in the frontal and parietal lobes.

The significant relationship between GM volume and the log of age in the frontal and parietal GM supraregions (see $t(\beta)$ in Table III) indicated that these regions experienced a period of significant tissue loss in adolescence, which decelerated in the second decade. However we did not observe a significant relationship between age and the volumes of the temporal, occipital, or limbic GM supraregions. This is consistent with previous studies that have found that while the association cortices undergo significant structural changes during adolescence and beyond [Pfefferbaum et al., 1994;

Steen et al., 1997; Thompson et al., 2001], maturation of the evolutionary older limbic structures is largely complete by this time [Sowell et al., 1999], as is maturation of the primary sensory cortices [Huttenlocher, 1999], which constitute a large proportion of the temporal and occipital lobes. These results indicate that the time-course of gray matter maturation is heterogeneous across the brain.

Previous studies have indicated that rather than being due to neuron death, adolescent gray matter loss may rather be due to a programmed reduction in synapses and their associated neuropil, i.e., dendrites, dendritic spines, and axon terminals. There is evidence that a dramatic synaptic prune occurs in healthy adolescence in the cortex of both humans [Huttenlocher and Dabholkar, 1997] and primates [Rakic et al., 1986]. Indeed, Bourgeois and Rakic [1993] used an electron micrograph to count the number of synapses in the visual cortex of macaque monkeys between the ages of 2.7 and 5 years (the period corresponding to adolescence) and estimated that they were losing up to 5,000 synapses per minute over this period. In light of the fact that late adolescence and early adulthood is the most common time for the onset of schizophrenia, a number of theorists have suggested that schizophrenia is caused by an abnormality in this synaptic prune [Feinberg, 1982; Hoffman and Dobscha, 1989; McGlashan and Hoffman, 2000]. Support for this theory comes from the fact that while patients with schizophrenia have a similar total number of neurons compared to controls [Feinberg, 1982; Pakkenberg, 1993; McGlashan and Hoffman, 2000], they show increased neuronal density, i.e., an increased number of neurons per unit of cortical volume [Selemon and Goldman-Rakic, 1999]. This finding is consistent with a reduction in cortical volume, possibly resulting from a reduction in the volume of neuropil in patients with schizophrenia [Selemon and Goldman-Rakic, 1999].

In contrast to the reductions in frontal and parietal GM volume, white matter volume was observed to increase curvilinearly (i.e., with the log of age) in only the parietal lobe, although the β -values for the frontal, temporal, and occipital WM regions were close to significance at $\alpha = 0.01$ (Fig. 4, Table III). This result further supports the idea that the association cortices undergo significant change in adolescence and early adulthood, with some studies finding that

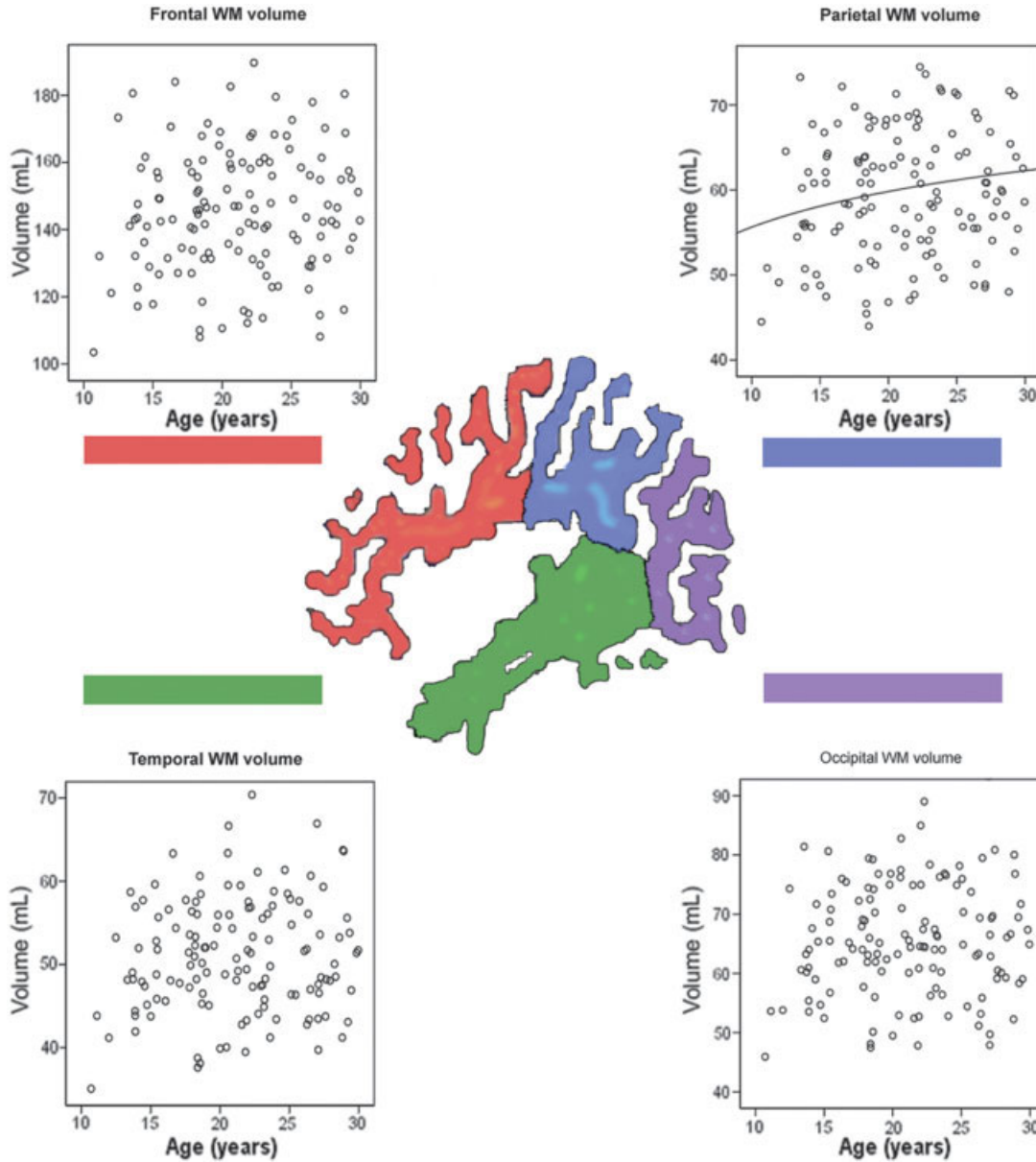


Figure 4.

White matter vs. age scatterplots for the frontal lobe, parietal lobe, occipital lobe, and temporal lobe regions of interest.

myelination of the association cortices is not complete until the late 20s [Yakovlev and Lecours, 1967]. Previous research, however, has suggested that the rapid change that is present in adolescent GM development is not present in adolescent WM development, but rather that WM increases smoothly from birth, but at a decreasing rate with age [Pfefferbaum et al., 1994]. An abnormality in adolescent myelination has also been proposed to be associated with the development of schizophrenia [Lim et al., 1998]. Given the role that myelin plays in modulating axonal conduction velocities, this hypothesis is especially salient in light of theories that empha-

size the role of neural timing in the development of disorganized thinking [Andreasen et al., 1999].

Corresponding to our observed age-related reduction in gray matter volume, we observed a similar curvilinear reduction in absolute power in each of the four EEG regions across each of the three frequency bands (Table IV). This is consistent with our hypothesis that a reduction in gray matter (irrespective of whether it reflected an elimination of neurons or neuropil) would result in the elimination of synapses, which would lead to a reduction in amplitude of the EEG activity recorded at the scalp and thus a reduction

in absolute EEG power. Although the curvilinear reduction in power with age was statistically significant for all three frequency bands, the relationship was far stronger, and mirrored the gray matter reduction better, in the slow-wave frequency band as compared to the alpha or beta bands. We can speculate as to why this might be.

The slow-wave frequency band is thought to arise primarily from highly synchronous local neural activity between cortical (pyramidal) neurons. This synchrony is responsible for the large amplitudes (and thus the large power) associated with slow-wave activity. Thus, a large reduction in the number of synapses involved in slow-wave activity would be expected to result in a considerable loss of power. The beta frequency band, on the other hand, is thought to arise primarily from asynchronous activity between cortical pyramidal neurons and is associated with low EEG power compared to the slow-wave band. This asynchrony implies that the elimination of synapses involved in beta activity might actually result in an increase in power if the pruned synapses were interfering destructively with others in the vicinity. Thus, it is possible that the relationship between synapse number and absolute power does not hold true for the high-frequency neural activity. Alternatively, the low amount of power associated with beta activity could result in any relationship with gray matter volume being indistinguishable from background variation, i.e., insufficient signal to noise. The alpha frequency (8–13 Hz), on the other hand, is thought to be quite distinct from all other brain frequencies, the idiosyncratic alpha “peak” on a typical EEG power spectrum being a testament to this. While the other frequencies are thought to arise from the synchronous and asynchronous “chatter” between cortical neurons, alpha activity is thought to reflect highly synchronous cortical activity driven by the thalamus. Thus, alpha activity might be expected to be influenced by structural changes in the thalamus, or thalamocortical relays, more so than changes in cortical gray matter per se. An alternative, and arguably more parsimonious, explanation lies in the fact that the occipital lobe (where alpha power is characteristically largest) did not show significant age-related changes in GM volume. Thus, even if the hypothesized relationship between the number of synapses and EEG power held in the alpha frequency band, alpha would not be expected to show as predictable an age-related decrease in power in comparison to the slow-wave band, which has a more homogeneous spatial distribution.

Given the novelty of this research, these results (and the conclusions drawn from them) should be treated with caution until they are replicated. It would be useful to replicate this study using a more exact nonlinear spatial normalization procedure [e.g., Christensen et al., 1996] than the one applied here. It would also be beneficial to replicate these results using a nonparametric MRI analysis technique [e.g., Bullmore et al., 1999], which makes fewer assumptions of the data than the method described above. We are also aiming to incorporate the LORETA [Pascual-Marqui et al., 1994] EEG source-localization technique into the analysis

procedure, as it would provide a finer-grained approach to mapping the EEG signal to the underlying neuroanatomy than the method employed in this study.

In conclusion, this study found evidence of significant structural brain change in adolescence and early adulthood. Gray matter was observed to decrease at a decreasing rate in the frontal and parietal cortices, while white matter was observed to increase at a decreasing rate in the parietal lobe across the age range of 10 to 30 years. We also observed curvilinear reductions in cortical EEG power, which mirrored the decreases in cortical gray matter, especially for the slow-wave frequencies. We suggest that this reduction in EEG power is caused by a developmental period of synaptic pruning that occurs in healthy adolescence.

ACKNOWLEDGMENTS

The authors thank Braddon Lance from the Department of Statistics, Macquarie University, New South Wales, Australia, for his advice on the statistical analyses. The authors acknowledge the Brain Resource International Database for its support in regards to the acquisition of the normative data [<http://www.brainresource.com>].

REFERENCES

- Andreasen NC, Nopoulos P, O’Leary DS, Miller DD, Wassink T, Flaum M (1999): Defining the phenotype of schizophrenia: cognitive dysmetria and its neural mechanisms. *Biol Psychiatry* 46:908–920.
- Ashburner J, Friston KJ (2000): Voxel-based morphometry: the methods. *Neuroimage* 1:805–821.
- Ashburner J, Friston KJ (2001): Why voxel-based morphometry should be used. *NeuroImage* 14:1238–1243.
- Benes FM (1989): Myelination of cortical-hippocampal relays during late adolescence. *Schizophr Bull* 15:585–593.
- Benes FM, Turtle M, Khan Y, Farol P (1994): Myelination of a key relay zone in the hippocampal formation occurs in the human brain during childhood, adolescence, and adulthood. *Arch Gen Psychiatry* 51:477–484.
- Bourgeois JP, Rakic P (1993): Changes of synaptic density in the primary visual cortex of the macaque monkey from fetal to adult stage. *J Neurosci* 13:2801–2820.
- Bullmore ET, Suckling J, Overmeyer S, Rabe-Hesketh S, Taylor E, Brammer MJ (1999): Global, voxel and cluster tests, by theory and permutation, for a difference between two groups of structural MR images of the brain. *IEEE Trans Med Imaging* 18:32–42.
- Christensen GE, Rabbitt RD, Miller MI (1996): Deformable templates using large deformation kinematics. *IEEE Trans Image Process* 5:1435–1447.
- Dustman RE, Shearer DE, Emmerson RY (1999): Life-span changes in EEG spectral amplitude, amplitude variability and mean frequency. *Clin Neurophysiol* 110:1399–1409.
- Feinberg I (1982): Schizophrenia: caused by a fault in programmed synaptic elimination during adolescence? *J Psychiatr Res* 17:319–334.
- Gasser T, Verleger R, Bacher P, Sroka L (1988): Development of the EEG of school-age children and adolescents: I, analysis of band power. *Electroenceph Clin Neurophysiol* 69:91–99.
- Giedd JN, Blumenthal J, Jeffries NO, Castellanos FX, Liu H, Zijdenbos A, Paus T, Evans AC, Rapoport JL (1999): Brain development

- during childhood and adolescence: a longitudinal MRI study. *Nat Neurosci* 2:861–863.
- Good CD, Johnsrude I, Ashburner J, Henson RNA, Friston KJ, Frackowiak RSJ (2001): A voxel-based morphometric study of aging in 465 normal adult human brains. *NeuroImage* 14:21–36.
- Gratton G, Coles M, Donchin E (1983): A new method for the off-line removal of ocular artifact. *Electroencephalogr Clin Neurophysiol* 55:468–484.
- Hickie I, Hadzi-Pavlovic D, Scott E, Davenport T, Koschera A, Naismith S (1998): SPHERE: a national depression project. *Australas Psychiatry* 6:248–250.
- Hoffman RE, Dobscha SK (1989): Cortical pruning and the development of schizophrenia: a computer model. *Schizophr Bull* 15:477–490.
- Huttenlocher PR (1979): Synaptic density in human frontal cortex: developmental changes and effects of aging. *Brain Res* 163:195–205.
- Huttenlocher PR, Dabholkar AS (1997): Regional differences in synaptogenesis in human cerebral cortex. *J Comp Neurol* 387:167–178.
- Huttenlocher PR (1999): Dendritic and synaptic development in human cerebral cortex: time course and critical periods. *Dev Neuropsychol* 16:347–349.
- Keshavan MS, Anderson S, Pettegrew JW (1994): Is schizophrenia due to excessive synaptic pruning in the prefrontal cortex? the Feinberg hypothesis revisited. *J Psychiatr Res* 28:239–265.
- Lim KO, Adalsteinsson E, Spielman D, Sullivan EV, Rosenbloom MJ, Pfefferbaum A (1998): Proton magnetic resonance spectroscopic imaging of cortical gray and white matter in schizophrenia. *Arch Gen Psychiatry* 55:346–352.
- Matousek M, Petersen I (1973): Automatic evolution of EEG background activity by means of age-dependent EEG quotients. *Electroenceph Clin Neurophysiol* 35:603–612.
- Matsuura M, Yamamoto K, Fukuzawa H, Okubo Y, Uesugi H, Moriwa M, Kojima T, Shimazono Y (1985): Age development and sex differences of various EEG elements in healthy children and adults—quantification by a computerized wave form recognition method. *Electroenceph Clin Neurophysiol* 60:394–406.
- McGlashan TH, Hoffman RE (2000): Schizophrenia as a disorder of developmentally reduced synaptic connectivity. *Arch Gen Psychiatry* 57:637–648.
- Nagy Z, Westerberg H, Klingberg T (2005): Maturation of white matter is associated with the development of cognitive functions in childhood. *J Cog Neurosci* 16:1227–1233.
- Niedermeyer E, Lopes de Silva FH (1999): *Electroencephalography: Basic Principles, Clinical Applications and Related Fields*. Baltimore, MD: Lippincott Williams and Wilkins.
- Pakkenberg B (1993): Total nerve cell number in neocortex in chronic schizophrenics and controls estimated using optical disectors. *Biol Psychiatry* 34:768–772.
- Pascual-Marqui RD, Michel CM, Lehmann D (1994): Low resolution electromagnetic tomography: a new method for localizing electrical activity in the brain. *Int J Psychophysiol* 18:49–65.
- Paus T, Collins DL, Evans AC, Leonard G, Pike B, Zijdenbos A (2001): Maturation of white matter in the human brain: a review of magnetic resonance studies. *Brain Res Bull* 54:255–266.
- Pfefferbaum A, Mathalon DH, Sullivan EV, Rawles JM, Zipursky RB, Lim KO (1994): A quantitative magnetic resonance imaging study of changes in brain morphology from infancy to late adulthood. *Arch Neurol* 51:874–887.
- Purves D, Lichtman JW (1980): Elimination of synapses in the developing nervous system. *Science* 210:153–157.
- Purves D (1998): *Body and Brain: A Trophic Theory of Neural Connections*. Cambridge, MA: Harvard University Press.
- Rakic P, Bourgeois JP, Eckenhoff MF, Zecevic N, Goldman-Rakic PS (1986): Concurrent overproduction of synapses in diverse regions of the primate cerebral cortex. *Science* 232:232–235.
- Selemon LD, Goldman-Rakic PS (1999): The reduced neuropil hypothesis: a circuit based model of schizophrenia. *Biol Psychiatry* 45:17–25.
- Sisk CL, Foster DL (2004): The neural basis of puberty and adolescence. *Nat Neurosci* 7:1040–1047.
- Sowell ER, Thompson PM, Holmes CJ, Batth R, Jernigan TL, Toga AW (1999): Localizing age-related changes in brain structure between childhood and adolescence using statistical parametric mapping. *NeuroImage* 9:587–597.
- Steen RG, Ogg RJ, Reddick WE, Kingsley PB (1997): Age-related changes in the pediatric brain: quantitative MR evidence of maturational changes during adolescence. *Am J Neuroradiol* 18:819–828.
- Thatcher RW, Biver C, McAlaster R, Camacho M, Salazar A (1998): Biophysical linkage between MRI and EEG amplitude in closed head injury. *NeuroImage* 7:352–367.
- Thompson PM, Vidal C, Giedd JN, Gochman P, Blumenthal J, Nicholson R, Toga AW, Rapoport JL (2001): Mapping adolescent brain change reveals dynamic wave of accelerated gray matter loss in very early-onset schizophrenia. *Proc Natl Acad Sci U S A* 98:11650–11655.
- Tzourio-Mazoyer N, Landeau B, Papathanassiou D, Crivello F, Etard O, Delcroix N, Mazoyer B, Joliot M (2002): Automated anatomical labeling of activations in SPM using a macroscopic anatomical parcellation of the MNI MRI single-subject brain. *NeuroImage* 15:273–289.
- Yakovlev P, Lecours A (1967): The myelinogenetic cycles of regional maturation of the brain. In: Minkowski A, editor. *Regional Development of the Brain Early In Life*. Boston: Blackwell Scientific Publications. p 3–70.